Check for updates

Physical and oxidative stability of fish oil-in-water emulsions stabilized with emulsifier peptides derived from seaweed, methanotrophic bacteria and potato proteins

Betül Yesiltas [a],[*], Alyssa M. Soria Caindec [a], Pedro J. García-Moreno [a],[b], Simon Gregersen Echers [c], Tobias Hegelund Olsen [d], Nykola C. Jones [e], Søren V. Hoffmann [e], Paolo Marcatili [d], Michael T. Overgaard [c], Egon B. Hansen [a], Charlotte Jacobsen [a]

[a] National Food Institute, Technical University of Denmark, Denmark
[b] Department of Chemical Engineering, University of Granada, Spain
[c] Department of Chemistry and Bioscience, Aalborg University, Denmark
[d] Department of Bio and Health Informatics, Technical University of Denmark, Denmark
[e] ISA, Department of Physics and Astronomy, Aarhus University, Denmark

GRAPHICAL ABSTRACT
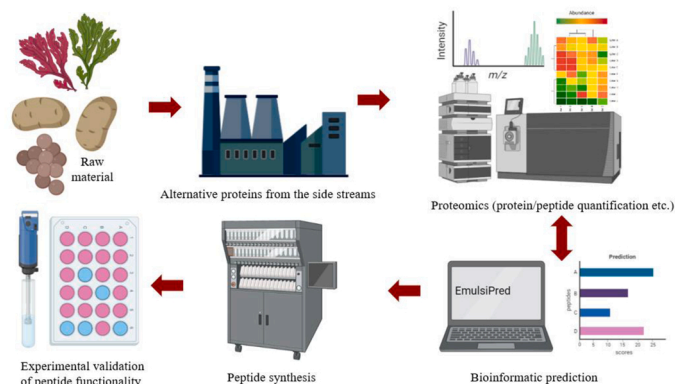
ARTICLE INFO

ABSTRACT

This study investigated the emulsifying and antioxidant activity of 10 peptides derived from seaweed, methanotrophic bacteria, and potatoes, which were identified as emulsifiers using quantitative proteomics and predictive bioinformatics. The factors (e.g., interfacial properties, secondary structure, net charge) behind the dual-functionality of peptides were characterized and related to peptides' ability to provide physical and oxidative stability in 5 % fish oil-in-water emulsions during 10 days of storage. The secondary structure of some of the peptides changed from highly disordered to more α-helical (GIIPATILEFLEGQLQEVDNNKDAR and GIIPGTILE-FLEGQLQK) or β-strand (VGFACSGSAQTYLSFEGDNTGRGEEEVAI, ELQVSARVTLEIEL, KVKINETVEIKGKFHV, RSPQKKESDMMKATKFAVVLMAAGLTVGCA) structures when adsorbed at the oil-water interface in comparison

to aqueous solution. The physical stability analyses confirmed that three seaweed peptides (IDSSFDSLPTDVVRVANSSCDAVE, VGFACSGSAQTYLSFEGDNTGRGEEEVAI, and ELQVSARVTLEIEL), one of the methanotrophic bacteria peptides (KVKINETVEIKGKFHV) and two of the potato peptides (GIIPATILE-FLEGQLQEVDNNKDAR and GIKGIIPAIILEFLEGQLQEVDNNKDAR) can indeed produce physically stable emulsions. The predicted emulsifier peptide embedded in methanotrophic bacteria protein (KVKINETVEIKGKFHV) outperformed all the samples in its ability to retard lipid oxidation in emulsions. This was evident as this sample had the lowest hydroperoxides formation (peroxide value < 10 meq O_2/ kg oil), tocopherols consumption, and volatile compound concentration, especially for t,t-2,4-heptadienal (14 ng/g sample) and 2-ethyl-furan (no formation). Non-enzymatic browning, which may indicate advanced stages of oxidation, occurred in all emulsions except for those stabilized with KVKINETVEIKGKFHV and sodium caseinate. Even though the positively charged peptides yielded better oxidative stability compared to negatively charged ones, there are several other factors (i.e., length, structure, charge, ability to decrease oil-water interfacial tension) affecting the physical and oxidative stability of emulsions. Therefore, it must be kept in mind that it is the collective action of these factors that ultimately define the functionality of peptides. In its entirety, KVKINETVEIKGKFHV proved to be highly effective in its technological functions as an emulsifier and antioxidant.

1. Introduction

Processed foodstuffs typically exist in the form of complex, multi-phase, and multicomponent colloidal systems. Emulsifiers are the key molecules that facilitate the formation and stabilization of these structures during processing [16]. Although many of the most effective emulsifiers currently used in food products are synthetic, such as sorbitan esters, fatty alcohol ethoxylates, and sucrose esters [31,37,60], there is a growing demand for the use of natural and sustainable ingredients in food products due to increasing awareness about healthy eating and environmental sustainability [39,9]. In this pursuit, there has been a recent interest to identify and characterize emulsifier peptides derived from alternative protein sources such as plants, marine, and microbial origin as well as side streams from the food industry [11,25, 24,29,6,64]. Emulsifier peptides may also contribute to enhancing the oxidative stability of emulsions (e.g., fish oil-in-water emulsions), where lipid oxidation is decreased during processing and storage [35,65]. Moreover, the study of antioxidant peptides from foods, plants, and animals has garnered much attention in several industries (e.g. pharmaceutical, alimentary health, processing/preservation) [54,62]. In food systems, these food-derived antioxidants are deemed safer and free from side effects associated with synthetic antioxidants [62].

In a recent study we showed that peptides embedded in proteins from red seaweed, single cell and potato showed emulsifying properties [64]. The seaweed and potato proteins can be obtained as side-streams from carrageenan and potato starch production and could thus serve as an untapped resource of natural emulsifier [24,29]. In our previous studies, quantitative proteomics and predictive bioinformatics were used as time and cost effective tools to identify emulsifier peptides embedded within highly abundant proteins from seaweed, methanotrophic bacteria, and potato sources using EmulsiPred (https://github.com/MarcatiliLab/E mulsiPred) [25,29,64]. In order to form stable emulsions, the protein/peptide must adsorb at the oil-water interface and thereby reduce the interfacial tension. As a result, the emulsifying capacity of peptides depend on a balance of hydrophilic and lipophilic properties [28]. Through different structural conformations upon adsorbing at the interface, peptides can exhibit emulsifying properties [15]. Moreover, based on their secondary structure, peptides can be categorized as the following: i) alpha, which are predicted to have α-helix structure, hence, have facial amphiphilicity, ii) beta, which are predicted to have beta-strands as the constituents of β-sheets, hence, facial amphiphilicity [21,53] iii) gamma, which are predicted to have perpendicular amphiphilicity [25].

In the present work, a set of the best performing peptides embedded in seaweed, methanotrophic bacteria and potato proteins was selected and evaluated for their potential dual-function role in emulsions as an emulsifier and antioxidant. Specifically, this study aimed at: i) investigating conformational changes in the secondary structure of the selected emulsifier peptides when adsorbed at the oil/water interface, and ii)

evaluating the physical and oxidative stability of 5 % fish oil-in-water emulsions stabilized the emulsifier peptides during 10 days of storage. High pressure homogenization, as a way to mimic industrial emulsion production, as well as advanced analytical methods to determine lipid oxidation (e.g. GC-MS to measure secondary volatile oxidation products) were used in this work, which aids the use of the results for new food applications. Overall, functional peptides embedded within parent proteins from seaweed, methanotrophic bacteria, and potato have been particularly investigated, serving as economical and readily available sources of protein.

2. Materials and methods

2.1. Materials

Synthetic peptide samples having a purity of > 70 % were obtained from ChinaPeptides Co., Ltd. (Shanghai, China). The information about the peptides: amino acid (AA) sequence, length, and net charge at pH 7 can be seen in Table 1. Peptides were kept at $- 20\,^\circ$C until use. S, U and P denote that its origin is from seaweed, methanotrophic bacteria and potato, respectively. The sample codes were kept similar to the previous screening tests performed by Garcia-Moreno, Gregersen, et al. (2020) and Yesiltas, Gregersen et al. [64], with a, b and g denoting that the peptides were predicted to adopt α-helical or β-strand secondary structure, or adsorb perpendicularly at the interface (γ), respectively. The net charge at pH 4 and 7, and isoelectric point (pI) were calculated using peptide property calculator from Innovagen (Innovagen AB, Lund, Sweden). The molecular weight of the peptides was provided by ChinaPeptides on their Certificate of Analysis. Commercial cod liver oil was provided by Vesteraalens A/S (Sortland, Norway) and kept at $- 40\,^\circ$C until use. The fatty acid (%, w/w) composition of the fish oil was as follows: C14:0 (0.2 %), C16:0 (9.4 %), C16:1 n-7 (8.6 %), C18:0 (2.0 %), C18:1 n-9 (16.2 %), C18:1 n-7 (4.6 %), C18:2 n-6 (1.8 %), C18:3 n-3 (0.1 %), C20:1 n-9 (12.6 %), C20:5 n-3 (9.1 %), C22:1 n-11 (5.9;%) and C22:6 n-3 (11.1 %). It had a peroxide value (PV) of 0.14 ± 0.01 meq O_2/kg oil. The tocopherols content of the fish oil was 168.26 ± 3.19 μg toc/g oil, 6.88 ± 0.40 μg toc/g oil, 100.29 ± 2.93 μg toc/g oil, 8.90 ± 0.65 μg toc/g oil, for alpha, beta, gamma, and delta, respectively. Sodium caseinate (cas) (Miprodan 30), which was used as a control with excellent emulsifying activity, was provided by Arla Foods amba (Viby J, Denmark).

2.2. Peptide secondary structure determination using Synchrotron Radiation Circular Dichroism (SRCD) spectroscopy

The secondary structure of peptides was determined using SRCD spectroscopy by the analysis of peptides both in solution and 5 % tricaprylin oil-in-water emulsions. 0.2 wt% peptide solutions were prepared by dissolving peptides in 10 mM phosphate buffer at pH7 first

shaking at 100 rpm for 2 h in a water bath at 50 °C, followed by shaking overnight at room temperature for complete rehydration. Production of the 5 % oil-in-water emulsions were described in detail by García-Moreno et al. [26]. Briefly, two step homogenization was used, first with primary homogenization mixing at 18,000 rpm for 30 s by using a POLYTRON® PT1200E (Kinematic Inc., New York, USA) followed by the secondary homogenization using a sonicator equipped with a P1 probe at an amplitude of 75 % (maximum amplitude of 180 µm), running 2 passes of 30 s with a break of 1 min between passes (Microson XL2000, Misonix, Inc., New York, USA). Sodium dodecyl sulfate (SDS) was used in the same conditions as peptides for the baseline correction. SRCD measurements were performed at the AU-CD beamline at the ASTRID2 synchrotron radiation source (ISA, Department of Physics & Astronomy, Aarhus University, Denmark). The operation of the SRCD spectrometer was confirmed using camphorsulfonic acid for optical rotation magnitude and wavelength on a daily basis [46]. A 0.01 cm path length quartz Suprasil cell (Hellma GmbH & Co., Germany) was used for far-UV SRCD measurements at 25 °C. The baseline was corrected using measurement of 10 mM phosphate buffer (pH 7) for peptide solutions and SDS stabilized tricaprylin-in-water emulsion for peptides-stabilized emulsions, as previously described [26]. The far-UV SRCD spectra were recorded in triplicate from 280 to 170 nm in 1 nm steps, with a dwell time of 2 s per point.

2.2.1. SRCD data analysis and calculation of peptides' secondary structure

The spectra were converted to delta epsilon units using the peptide concentration obtained from absorbance at 205 nm and corrected for scattering where necessary [47]. When light is elastically scattered from particles with a size similar to or smaller than the wavelength, it may not be detected. Where scattering occurs is evident in the absorbance spectrum which is measured simultaneously with the CD spectrum. A long and non-zero sloping tail of the absorbance curve can be fitted using an equation based on Rayleigh scattering for simulating the effect of scattering over the full spectrum [47], allowing for a corrected absorbance at 205 nm to be obtained. The sequence of peptides was used to determine the molar extinction coefficient and mean residual weight [4]. Light scattering in emulsions leads to a change in the underlying CD baseline due to the very different paths of light through emulsion compared to solutions. To correct the baseline for this, the SDS stabilized emulsion was produced in the same way as for the peptides to enable reproduced light scattering [26]. The proportions of each secondary structure components were determined using a web-based calculation server DICHROWEB that incorporates various methods and a wide range of protein spectral databases [63]. The calculation method used in this study was CDSSTR with the reference set SMP180 [1,59]. Due to the differences in nature of the emulsions and solutions, due to the scattering at the oil droplets, the accuracy of peptide concentration determination is lower in emulsions than for those in solution [26]. However, the relative changes determined in the structure are still valid even though the higher uncertainties for emulsions, which may affect the absolute values obtained through the secondary structure fitting.

2.3. Storage experiment with 5 % fish oil-in-water emulsions

2.3.1. Emulsion production

First, the aqueous phases were prepared by dissolving (0.2 wt%) 0.44 g peptide or cas in 208.56 g buffer containing 10 mM sodium acetate and 10 mM imidazole [24,26]. All the samples were subjected to a water bath of 50 °C for 2 h and afterwards left for overnight stirring at room temperature. Due to the occurrence of cloudy aqueous phases for some peptides (80-s-a, 83-s-a, 104-p-g), all samples were treated with an ultrasonic bath (Cole-Parmer 8893, Illinois, USA) until they were solubilized (around 15 min) to facilitate solubilization. The pH of the samples was measured and adjusted to pH 7. Pre-homogenization was done using Ultra-turrax (Ystral GmbH, Dottingen, Germany) at 16,000 rpm for 3 min, with oil being added at the first minute. Homogenization was carried out using Microfluidizer (Gea Niro Soavi SpA, Parma, Italy) at 9 kpsi for 3 passes. The emulsion yield was too low for 80-s-a and 83-s-b due to instrument blockage and hence, the small amount of obtained emulsions were discarded. A 10 % sodium azide preservative solution was added to the emulsions to achieve a 0.05 wt% final concentration of the sodium azide. Iron (II) sulfate pro-oxidant solution, which was prepared at the same day of emulsion production, was added at 113 µL per 100 g emulsion to achieve 50 µM concentration in the final emulsion. The final emulsions were put into Pyrex media bottles and the pH was measured for a second time. Before storage at room temperature under darkness, the emulsions were divided as follows: 20 g aliquots for peroxide value determination and 15 g aliquots for volatile compounds determination, both of which were placed in separate amber bottles. At each time point, the emulsions were subsampled, and aliquots were stored at − 40 °C until analysis. The remaining emulsion volumes were kept for physical stability determinations and left to stand at room temperature in darkness.

2.3.2. Physical stability of emulsions

The emulsions were analyzed for droplet size distribution and changes in physical stability over 10 days of storage.

2.3.2.1. Droplet size distribution.
The droplet size distribution of the emulsions was measured on days 1, 3, 10 by laser diffraction using a Mastersizer 2000 (Malvern Instruments, Ltd., Worcestershire, UK) in recirculating water at 3000 rpm until it reached an obscuration of 12–15 %. Refractive indices of sunflower oil as the particle (1.469) and water (1.330) as dispersant were used and results were expressed as $D_{4,3}$. Triplicate measurements were performed.

2.3.2.2. Observation of physical instabilities.
Emulsion instability can be observed as oil droplets gather at the top of the emulsion. Although there is no clear water phase at the bottom of these emulsions, oil droplets can move upwards due to density difference between two liquids, e.g., water and oil. This indicates that destabilization is in progress. The oil rich phase index (OI) was calculated as follows: $OI = \frac{h_o}{h_t} * 100$, where h_t is the total height (cm) of the emulsion and h_o is the height (cm) of the

Table 1
Peptide codes, amino acid (AA) sequence, length, net charge (z) at pH 7, isoelectric point (pI), molecular weight (MW) and amphiphilic score.

Peptide	AA sequence	Length	z (pH 7)	pI	MW (Da)	Score[*]
80-s-a	IGYTVRNSLRVTVRDLSNLGLILDALVR	28	2.0	10.84	3127.68	3.30
82-s-a	IDSSFDSLPTDVVRVANSSCDAVE	24	-4.1	3.18	2526.72	3.28
83-s-b	RAGSNSLSRISFGISNEADLRDQAR	25	1.0	10.24	2720.95	3.18
84-s-b	VGFACSGSAQTYLSFEGDNTGRGEEEVAI	29	-4.1	3.44	2995.19	2.75
86-s-b	ELQVSARVTLEIEL	14	-2.0	3.85	1599.85	5.43
97-u-b	KVKINETVEIKGKFHV	16	2.1	10.24	1869.24	5.07
103-u-g	RSPQKKESDMMKATKFAVVLMAAGLTVGCA	30	2.9	10.22	3169.85	4.96
104-p-g	GIIPATILEFLEGQLQEVDNNKDAR	25	-3.0	3.79	2784.12	3.69
105-p-g	GIIPGTILEFLEGQLQK	17	-1.0	4.15	1856.20	2.45
g1	GIKGIIPAIILEFLEGQLQEVDNNKDAR	28	-2.0	4.16	3094.56	4.15

[*] Predicted amphiphilic scores are referred to previously published articles from our lab [25,64].

separated oil phase at the top of the emulsion.

2.3.3. Oxidative stability of emulsions

For peroxide value (PV), tocopherols content, and volatile compound determination, emulsions were stored at room temperature in darkness for a period of 10 days. The respective analyses were performed on days 0, 1, 3, 7, 10. The color changes of the samples were also investigated on day 10.

2.3.3.1. Determination of peroxide value.
Lipids were extracted using Bligh and Dyer method with some modifications [8]. Two lipid extracts were made for each emulsion. The PV of the lipid extracts was determined using the colorimetric ferric-thiocyanate method at 500 nm as described by Shanta and Decker [56]. Two 1 g aliquots of each extract were used for this analysis. Measurements were carried in duplicate, and data were expressed as milliequivalents of peroxides per kg of oil.

2.3.3.2. Tocopherols.
Tocopherols content was measured using high-performance liquid chromatography (HPLC) (Agilent 1100 Series, Palo Alto, CA, USA). Two 2 g aliquots of each abovementioned lipid extract were prepared and evaporated under nitrogen. The remaining oil was dissolved in 1 mL n-heptane and sealed in amber injection bottles. Afterwards, 40 µL of the sample was injected onto a Waters Spherisorb column (5 µm Silica; 250 × 4.6 mm) (Phase Separation Ltd., Deeside, UK). Elution was performed with an isocratic mixture of n-heptane/2-propanol (100:0.4, v/v) at a 1 mL/min flow and 20 µL injection volume into a column (Waters Spherisorb 3 µm Silica, 4.6 mm I.D. × 150 mm), preceded by a guard column (Waters Spherisorb, 5 µm Silica, 4.6 mm I. D. ×10 mm). Detection was carried out using a fluorescence detector with excitation at 290 nm and emission at 330 nm, as described in AOCS Official Method Ce 8-89. Measurements were carried in duplicate, and data were expressed in µg toc/g oil.

2.3.3.3. Volatile secondary oxidation products.
The secondary oxidation products from the emulsions were determined using dynamic headspace desorption followed by gas chromatography-mass spectrometry (GC-MS). Four g of emulsions were poured into a purge bottle. Approximately 5 mL distilled water and 30 mg of an internal standard (4-methyl-1-pentanol) was added. The purge bottles were subjected to a water bath 45 °C for 30 min under purging with nitrogen (150 mL/min) and the volatile compounds were trapped in Tenax GR tubes. Afterwards, the tubes were put into Automatic Thermal Desorber (ATD-400, Perkin Elmer, Norwalk, CN), which led to a gas chromatograph (GC) (HP 589 + IIA, Hewlett Packard, Palo Alto, CA, USA; Column: DB-1701, 30 m × 0.25 mm × 1.0 µm). The oven program had an initial temperature of 45 °C for 5 min, increasing with 1.5 °C/min until 55 °C, with 2.5 °C/min until 90 °C, and with 12.0 °C/min until 220 °C, where the temperature was kept for 4 min. The individual compounds were detected by mass spectrometry (MS) (HP 5972 mass-selective detector, Agilent Technologies, USA; electron ionization mode, 70 eV; scan range from 30 to 250 m/z) identified by MS-library searches (Wiley 138K, John Wiley and Sons, Hewlett-Packard). The identified volatiles were quantified by doing a 9-point standard curve (0.1–250 µg/mL standard) with external standards (in rapeseed oil) and each dilution of standards was added into the sodium caseinate emulsion and were analyzed the same way as the emulsion samples. sodium caseinate emulsion. The selected standards were 2-ethyl furan, 1-penten-3-one, pentanal, 1-penten-3-ol, 2,3-pentanedione, 1-pentanol, hexanal, heptanal, c-4-heptenal, benzaldehyde, octanal, t,t-2,4-heptadienal, and t,t-2,4-decadienal. Measurements were carried out in triplicate and were expressed in ng/g sample.

2.3.3.4. Colorimetry.
The color (CIE * L * a * b color space) of the emulsions was measured based on their absorbance at day 10 using Minolta Chroma Meter 200 (Konica Minolta Sensing Americas, Inc., New Jersey, USA) to determine the extent of browning of the emulsions during storage. Measurements were carried out in triplicate and results are expressed as *L, *a, *b values.

2.4. Statistical analysis

Multiple sample comparison was conducted using STATGRAPHICS Centurion (Statistical Graphics Corp., Rockville, MD, USA) with a 95 % significance level. Tukey's range test was used for post-hoc analysis to determine which variable(s) differed significantly. Data were expressed as means ± standard deviations (SD).

3. Results and discussion

3.1. Secondary structure of the peptides

Synchrotron radiation circular dichroism (SRCD) spectroscopy provides a great opportunity to work with complex emulsion systems. While the presence of highly absorbing non-chiral components, such as lipids and buffers, makes it difficult to perform measurements using bench-top CD instrumentation, the higher flux of the light from a synchrotron allows higher penetration leading to higher signal-to-noise ratio, which leads to obtaining more accurate results [45].

Peptides adsorbed at an oil/water interface commonly change their conformation and adopt a different secondary structure to expose their hydrophobic parts to the oil phase [21]. According to Dexter and Middelberg [15], facial amphiphilicity allows the peptides to orientate parallel to the interface rather than perpendicularly, which is typical for conventional surfactants. This allows the maximum number of interpeptide contacts to form, thereby strengthening the interfacial layer and yielding optimal functionality. This configuration can be achieved using both α-helix and β-strand secondary structures. In an α-helix, there is a periodicity of 3.6 residues per turn. Consequently, if hydrophobic residues are positioned in a way where they are three or four residues apart, the peptide will form a single hydrophobic site in the helical conformation which can interact directly with a hydrophobic phase (i.e., oil) at the oil-water interface. The hydrophilic residues on the opposite face of the helix will orientate towards the bulk aqueous phase. In β-strands, alternating hydrophobic and hydrophilic residues are adequate to form distinct molecular faces. In contrast to helical emulsifier peptides, where little or no interpeptide interactions are observed at the interface, interactions between adjacent strands through hydrogen bonds contribute to stabilizing the interfacial layer of β peptides [26]. Another potential type of peptides predicted by bioinformatics, gamma peptides, are those with hydrophobic and hydrophilic halves, which could orientate perpendicularly to the interface.

The far-UV SRCD spectra obtained for the peptides in solution and at the oil/water interface in oil-in-water emulsions illustrate potential changes in the secondary structure between the two states (Fig. 1a–i). Peptide 80-s-a was not fully soluble and hence, SRCD spectra obtained for this peptide in solution are not fully reliable. Secondary structure changes for 80-s-a and 83-s-b at the oil-water interface could not be determined, as emulsions prepared with these peptides physically unstable before measuring. Thus, the resulting spectra were not reproducible and protein concentration in these emulsions could not be properly determined, therefore delta epsilon spectra could not be obtained.

Through spectral deconvolution, the secondary structure composition (% α-helix, β-strand, turns, and unordered) of peptides can be calculated in both systems (Fig. 2). The secondary structure of the peptides in solution was predominantly disordered, where turns and unordered accounts for between 44 % and 62 % of the structure for different peptides (Fig. 2a). Peptides 80-s-a and 86-s-b showed around 15 % α-helical structure in solution (Fig. 2a,e), with 80-s-a showing the expected negative peak at 222 nm, and 86-s-b showing the positive peak a 192 nm, which are indicative of α-helical structure [32]. Nevertheless,

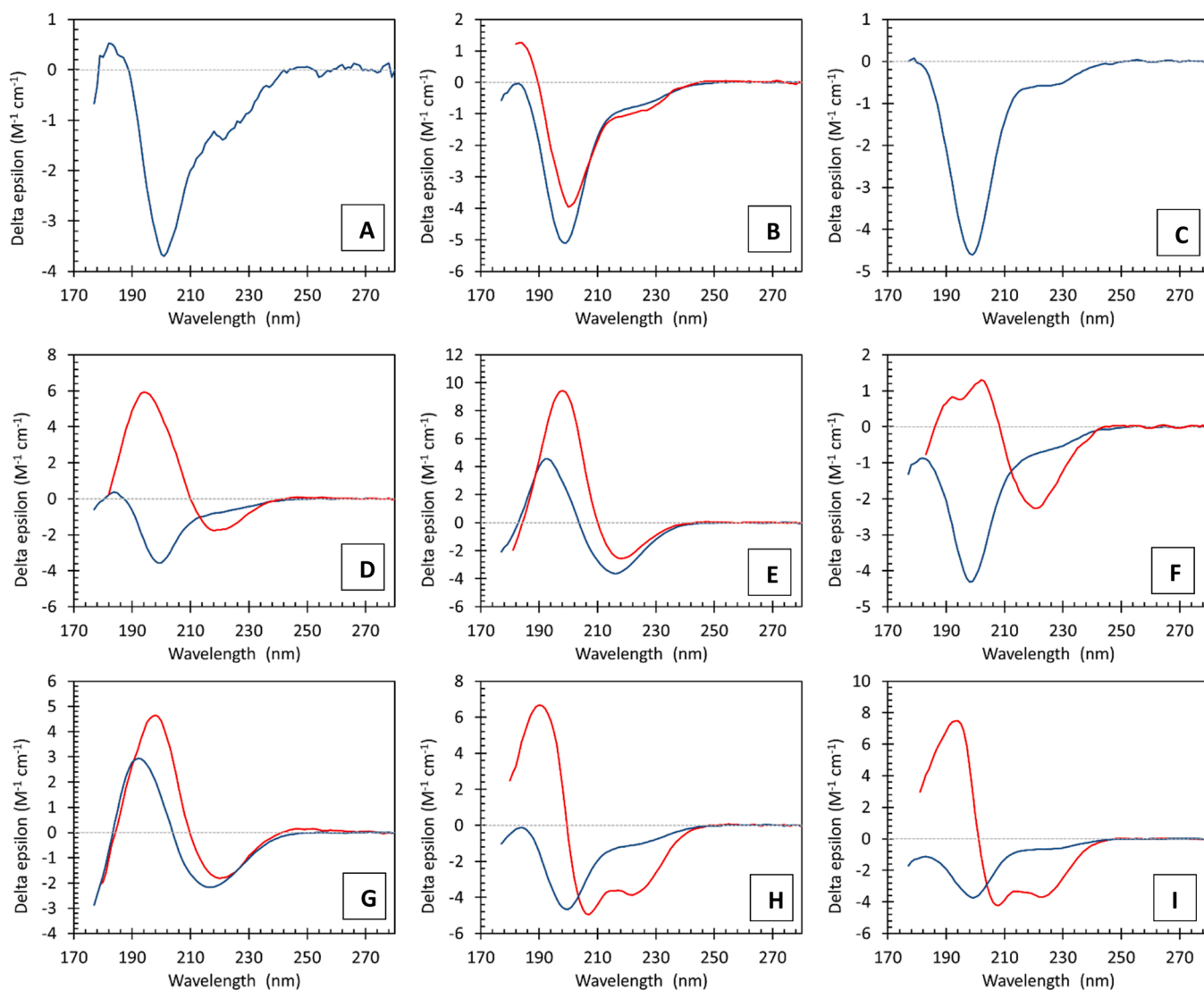**Fig. 1.** Far-UV SRCD spectra of peptides in solution at pH ~ 7 (blue line) and adsorbed at tricaprylin oil-water interface (red line): a) 80-s-a, b) 82-s-a, c) 83-s-b, d) 84-s-b, e) 86-s-b, f) 97-u-b, g) 103-u-g, h) 104-p-g, and i) 105-p-g. Light scattering of oil droplets in the casein- or peptides-stabilized emulsions was corrected using SDS-stabilized emulsions.

all peptides in solution, including these 2 peptides, obtained a higher percentage (around 30–40 %) of β-strand structure (Fig. 2a). These results are in line with previously studied emulsifier peptides [26].

Adsorption at the tricaprylin oil-water interface resulted in significant changes in their secondary structure for most peptides (Fig. 1). Far-UV spectra of the peptides in solution and in emulsion indicated that the secondary structure of the peptides 84-s-b, 86-s-b, 97-u-b, and 103-u-g gained in β-strand conformation by between 11 % and 35 %, when adsorbed at the o/w interface (Fig. 1d–g and Fig. 2). Indeed, these peptides, except 103-u-g, were predicted to adopt β-strand conformation at the oil/water interface, thus exhibiting the anticipated facial amphiphilicity. These findings agree with those found previously for β-strand predicted peptides [26] and align with the structure of the peptides when contained in the native protein [64]. On the contrary, peptides 104-p-g and 105-p-g significantly increased their α-helix conformation (to 45 % and 55 % respectively), when adsorbed at the oil-water interface compared to their conformation in solution (Fig. 1h,i and Fig. 2). Although these peptides were predicted to be emulsifiers through perpendicular amphiphilicity, this finding was not surprising, as these 2 peptides are variants of the γ-1 peptide, which was previously reported to adopt a highly helical conformation when adsorbed at the oil/water

[26]. Similarly, homology modeling of these peptides indicated that they constitute surface-exposed regions with a high α-helix conformation within their native proteins, confirming that native conformation is in many cases a good model for interfacial structure of the isolated peptides [26,64]. Nevertheless, peptide 82-s-a, predicted to be a potential helical emulsifier, slightly increased in β-strand conformation from solution to o/w interface (Fig. 1b and Fig. 2), thereby illustrating that the models are not always correct. In this case, it is also worth to note that homology model previously presented [64], was not of high quality due to the lack of a good protein template. As such, the modeled structure of the native protein may not accurately reflect the in vivo tertiary structure, why such should be used with caution.

3.2. Physical stability of emulsions

Peptides 80-s-a and 83-s-b did not form emulsions due to solubility issues observed, such as aggregation and clogging of the microfluidizer during secondary homogenization. However, the rest of the peptides provided emulsions after production. 80-s-a decreased oil-water interfacial tension (IFT) down to around 9 mN/m [64]; however, failed to produce a stable emulsion. It should be borne in mind that the IFT
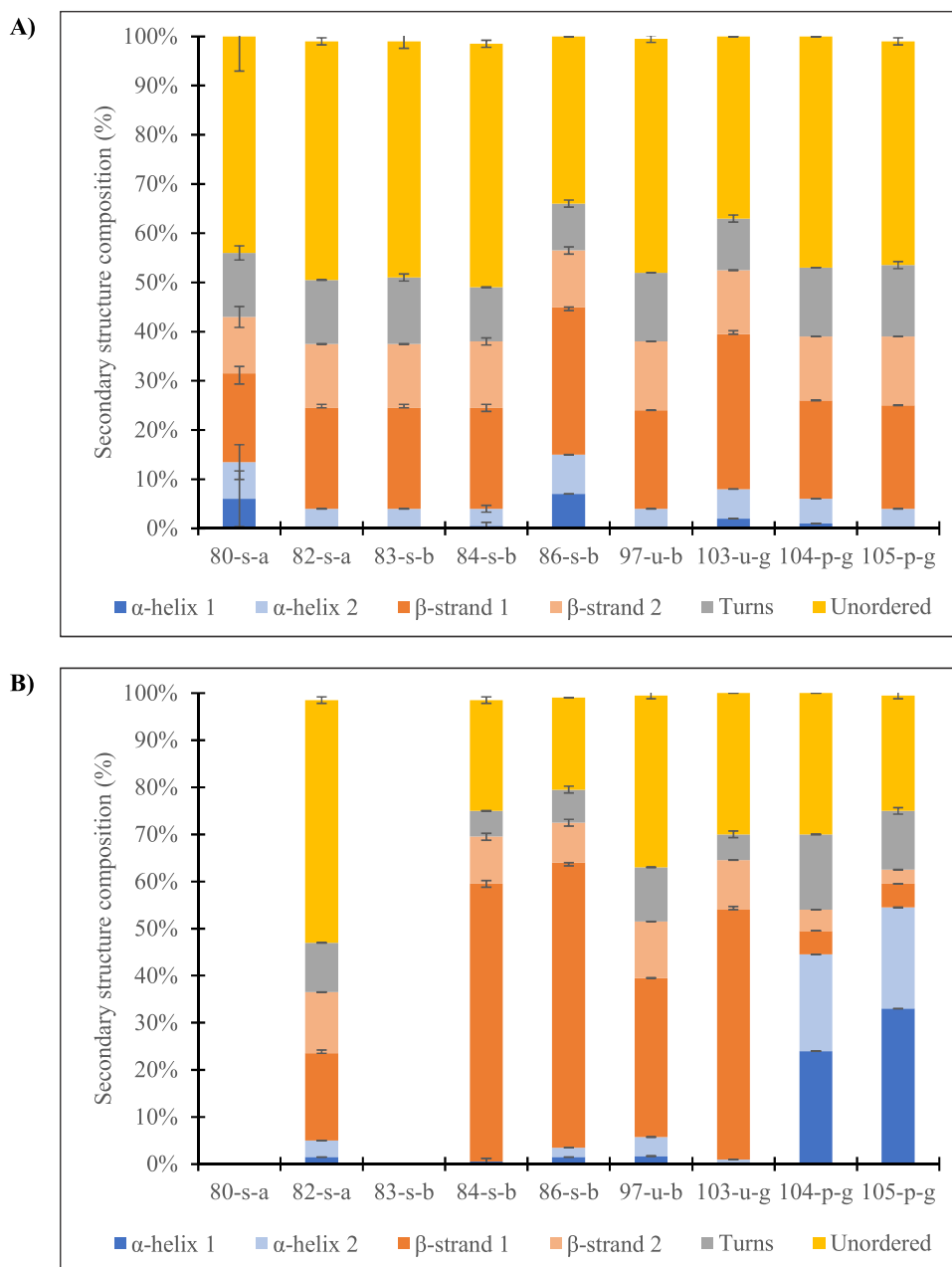
Fig. 2. The secondary structure composition (% α-helix, β-strand, turns and unordered) of peptides a) in solution, and b) adsorbed at tricaprylin-water interface. The results derived from deconvolution of the respective SRCD spectra. The numbers 1 and 2 in α-helix and β-strand denote regular and distorted structures, respectively.

Table 2
Values of droplet size and zeta potential of the emulsions stabilized with different peptides and sodium caseinate at specific days during storage at room temperature.

Sample	Zeta potential* (mV)	Volume moment mean diameter, $D_{4,3}$ (µm)			Surface moment mean diameter, $D_{3,2}$ (µm)		
		Day 1	Day 3	Day 10	Day 1	Day 3	Day 10
82-s-a	-53.7 ± 2.9	4.58 ± 0.22[d,x]	4.38 ± 1.41[bc,x]	4.45 ± 1.19[a,x]	0.204 ± 0.007[b,x]	0.245 ± 0.000[xy]	0.265 ± 0.033[bc,y]
84-s-b	-71.8 ± 3.5	0.29 ± 0.00[a,z]	0.28 ± 0.00[a,y]	0.27 ± 0.00[a,x]	0.147 ± 0.000[a,x]	0.147 ± 0.001[y]	0.144 ± 0.001[a,y]
86-s-b	-74.4 ± 2.8	0.54 ± 0.26[ab,x]	1.55 ± 0.28[ab,xy]	2.86 ± 1.38[a,y]	0.149 ± 0.002[a,x]	0.153 ± 0.005[xy]	0.155 ± 0.005[ab,x]
97-u-b	25.2 ± 1.9	0.33 ± 0.00[a,x]	1.56 ± 2.11[ab,x]	1.51 ± 0.70[a,x]	0.153 ± 0.000[a,x]	0.165 ± 0.009[xy]	0.178 ± 0.008[ab,y]
103-u-g	38.7 ± 2.7	0.79 ± 0.03[b,x]	0.81 ± 0.02[ab,x]	14.24 ± 6.51[b,y]	0.361 ± 0.022[c,x]	0.392 ± 0.026[xy]	0.836 ± 0.108[d,y]
104-p-g	-60.9 ± 3.0	2.05 ± 0.02[c,x]	1.86 ± 0.40[ab,x]	3.41 ± 0.57[a,y]	0.142 ± 0.000[a,x]	0.145 ± 0.001[y]	0.150 ± 0.001[a,z]
105-p-g	-59.3 ± 2.5	26.03 ± 0.01[e,x]	21.15 ± 3.10[d,x]	31.26 ± 1.60[c,y]	0.644 ± 0.025[d,x]	0.672 ± 0.004[xy]	0.752 ± 0.027[d,y]
g1	-62.4 ± 3.5	0.25 ± 0.00[a,x]	0.26 ± 0.01[a,x]	0.27 ± 5.30[a,x]	0.151 ± 0.000[a,x]	0.153 ± 0.002[x]	0.154 ± 0.001[ab,x]
Cas	-40.7 ± 1.7	0.42 ± 0.00[a,x]	6.00 ± 0.37[c,y]	17.12 ± 0.00[b,z]	0.199 ± 0.000[b,x]	0.244 ± 0.001[y]	0.317 ± 0.015[c,z]

Values are presented as mean ± sd (n = 9). Values followed by the same letter/s 'a–e' per column and 'x–z' per row are not significantly different (p ≤ 0.05).
*Zeta potential results are from a previous study published by our lab [24,64]. It should be noted that these results were measured on emulsions produced on a smaller scale using an ultraturrax and sonicator with the same emulsion formulation.

measurement is a static set up, whereas emulsion production is a dynamic system with high shear forces. Thus, total correlation between IFT and droplet size might not be observed. Low solubility of peptides (particles) may also lead to false IFT values [13]. This can be supported by the previous study stating that the 80-s-a provided a cloudy peptide solution at pH 7 [64].

The final pH of the emulsions ranged from 6.99 to 7.16 and were far from the isoelectric points of the respective peptides (Table 1), which is important as proteins and peptides have poor emulsion properties when near their isoelectric points [58]. Table 2 shows the zeta potential and the surface and volume weighted mean droplet sizes of 5 % fish oil-in-water emulsions containing the peptides of interest. Zeta potential measurements that denote an absolute electrical differential greater than 30 mV typically suggest higher colloidal stability and reduced tendency towards particle aggregation due to electrical repulsion [43]. According to Garcia-Moreno et al. [25], variations in zeta potential of the emulsions essentially stem from the net charge of the adsorbed peptides. In this case, due to the presence of some of the negatively charged amino acids (aspartic acid, D, and glutamic acid, E) at pH 7, emulsions stabilized with 82-s-a, 84-s-b, 86-s-b, 104-p-g and g1 had high negative zeta potential. These samples were among those that had the smallest droplet sizes, $D_{4,3}$, ranging between 0.27 and 4.45 μm after a 10-days storage (Table 2). Zeta potential is only one of the factors that contribute to the physical stability during storage. For example, emulsion stabilized with 86-s-b, 104-p-g, and 105-p-g also had high zeta potential values (< -59.3 mV); however, droplets were still aggregating during storage, which led to significant increase in droplet size (Table 2).

The small $D_{4,3}$ values, obtained and sustained during 10 days of storage by 84-s-b and g1, are in line with their high zeta potential values, -71.8 ± 3.5 and -62.4 ± 3.5 mV, respectively [24,64]. Indeed, 84-s-b and g1 were reported to have around 13.0 mN/m oil-water IFT when reached equilibrium as reported by García-Moreno et al. [24] and Yesiltas et al. [64], which is comparable to cas (11.8 mN/m when reached the equilibrium). The larger hydrophobic regions of g1 may have favored the interaction of the peptide with the oil at the interface, hence better physical stability and lower IFT. Moreover, it was noticeable that the $D_{4,3}$ of the emulsion stabilized with sodium caseinate (cas) kept rising significantly from day 0 to 10. Even though the zeta potential for cas was also sufficiently negative (-40.7 mV), which provided electrostatic repulsion and prevented creaming, oil droplets have aggregated over time. Although caseinate is an excellent emulsifier, it is not sufficient to totally stabilize the emulsions at the low concentration used here (0.2 wt%). This could possibly explain the increase in $D_{4,3}$ throughout storage.

Although 105-p-g was previously reported to have a highly negative surface charge (-59.3 mV) [64], it should be noted that this emulsion was unstable. It was clear that this was the only sample that manifested physical instability, specifically with an oil rich phase index, OI, of already 8.2 % after emulsion production (day 0) followed by 9.8 % on days 3 and 10. This physical instability can be confirmed with its large $D_{4,3}$ droplet size of 26.03 μm (already one day after production). 105-p-g only had 17 AA residues, and this may have lowered its potential to obtain an α-helical configuration at the interface and thereby resulted in insufficient emulsifying activity and emulsion stability. Although lower oil-water interfacial tension (IFT) values (11.1 mN/m) agree with better emulsifier action, 105-p-g emulsion demonstrated that the peptide was not able to reduce the interfacial tension to an extent where smaller droplets can be obtained as it was clearly observed that the emulsion was not stable throughout the storage [64] (Table S1, Supplementary material).

The emulsifying performance of peptides can be correlated to their structural characteristics (i.e., secondary structure conformation, amino acid sequence, and molecular weight). Overall, good physical stability (based on droplet size, surface charge and creaming stability) was obtained in emulsions stabilized with peptides adopting a predominant β-strand (84-s-b, 86-s-b, 97-u-b), or α-helical (104-p-g and g1) conformations at the oil/water interface. The emulsifying activity of these peptides was comparable with each other and resulted from an increased interaction between the oil and the hydrophobic parts of the peptides. Amphipathic α-helix is a structural feature which has been previously proposed to have enhanced emulsifying activity and high solubility [14, 57], as well as contributing to surface activity of protein by increased interaction between the oil and the hydrophobic parts [38,40]. This could explain the good emulsifying activity of the 104-p-g and g1 peptides as they were shown to obtain α-helical structure at the oil-water interface [26]. García-Moreno et al. [24] emphasized that α-peptides should have at least 18 AA residues and β-peptides around 13 AA residues to increase the potential of the peptides to adsorb at the interface. This finding clearly concurred with the results as the length of 86-s-b, 97-u-b, 104-p-g and g1 was in the range previously reported. On the other hand, 84-S-B, with 29 AA, resulted in emulsions with high physical stability when adopting a predominantly β-strand structure at the oil/-water interface. The latter suggests that 84-S-B has less tendency to form aggregates (i.e., when compared to other large β-peptides [25]) and thus properly diffuses and adsorbs at the interface.

Emulsions 97-u-b and 103-u-g had positive zeta potential values as expected [64], due to their positive net charge at pH 7 (Table 1). Although the zeta potential and creaming stability of the emulsion stabilized with 103-u-g seemed adequate indicating good physical stability, it had a significantly large increase in its $D_{4,3}$ and $D_{3,2}$ during storage (Table 2). This is in line with the high IFT value (18.2 mN/m) reported for this peptide (Table S1) [64] indicating that this peptide did not have greater ability to reduce the oil-water IFT during emulsification and thereby enabling the formation of smaller droplets, which lowers the tendency of droplet aggregation or coalescence [58]. Although 103-u-g adopted β-strand structure at the oil-water interface and had 30 AA residues, which was above the threshold for obtaining the secondary structure [25], this sample had significant increase in its $D_{4,3}$ at day 10 compared to day 3 indicating droplet aggregation.

Emulsion containing 97-u-b had a lower absolute zeta potential value (25.2 mV) compared to other emulsions and was clearly not among those that had the smallest IFT values (16.5 mN/m when reached the equilibrium) as reported by Yesiltas, Gregersen et al. [64] (Table S1), which correlated well with the increases observed in both $D_{4,3}$ and $D_{3,2}$ values of the emulsion from day 1 to 3, even though the initial droplet sizes were very small. However, it reduced the oil-water IFT and promoted droplet disruption sufficiently during homogenization, as the emulsion had low droplet sizes. Moreover, there was no significant increase in either of the droplet sizes from day 3 to 10, and physical instability was not observed. According to Ait-Akbour [2], it should be considered that the adsorption of the layers which increase emulsion stability sterically will lead to a lower zeta potential, which is, however, not an indication of a reduced physical stability. Stabilizer adsorption shifts the plain of shear (where the zeta potential is measured) to a larger distance from the particle surface and thereby lowers the measured zeta potential. In cases of combined electrostatic and steric stabilizers, a zeta potential of about -20 mV is enough to fully stabilize the system [5]. Moreover, 97-u-b has only 16 AAs. The smaller the molecular weight of an emulsifier, the faster the diffusion towards the interface [39,44,61]. Rapid adsorption of the emulsifier on the droplet surface is always advantageous because this enables rapid reduction of the interfacial tension, therefore preventing aggregation or coalescence [48]. However, the adsorption kinetics of the peptides cannot be singled out as the principal determinant of emulsion stability. It can also be advantageous to have larger peptides, such as g1, for obtaining a well-defined secondary structure at the interface. However, as the best performing peptides were both from shorter and larger ones, this shows the complexity of predicting the functionality based on a single characteristic such as size. Overall, based on several factors such as length, structure, charge, ability to decrease oil-water interfacial tension, peptides that showed the best emulsifying activities were 84-s-b, 86-s-b,

97-u-b, 104-p-g, and g1.

3.3. Oxidative stability of emulsions

Lipid autoxidation, a free radical-induced chain reaction, leads to the formation of fatty acid hydroperoxides, which then decompose to a wide range of secondary oxidation products. Some of these are volatile compounds with strong and negative flavor attributes, imparting the disagreeable characteristics and sensation of rancid fish oil [23]. Since polyunsaturated fatty acids (PUFAs) are highly susceptible to oxidation due to their degree of unsaturation (i.e. presence of double bonds), lipid oxidation is the most critical parameter affecting shelf life of fish oils and food products where marine lipids have been incorporated [18]. It is noteworthy that the use of peptides as emulsifiers, which could also exhibit antioxidant properties, is of high relevance. This is due to the fact that lipid oxidation is initiated at the o/w interface in emulsions, and thus having antioxidant activity localized at the interface, might be the most efficient approach to retard it [7].

3.3.1. Peroxide value

Fig. 3A shows the peroxide values (PV) of the emulsions prepared with different peptides and sodium caseinate as control. Table S2 in the Supplementary materials shows significant (p ≤ 0.05) differences between the samples and time points. At day 0, 104-p-g and g1 had already significantly higher PV at 25.23 meq O_2/ kg oil and 25.16 meq O_2/ kg

oil, respectively, than all the other emulsions, which were not significantly different from each other with PV ranging between 3.7 and 11.7 meq O_2/kg. This is in agreement with the results in a previous study on potato peptides, which also observed poor oxidative stability of emulsions prepared with these two peptides [26]. It was reported that the homogenization process can potentially be prooxidative due to high shear stress and incorporation of oxygen during emulsification [33] and the emulsions stabilized with the peptides 104-p-g and g1 were the least oxidatively stable during homogenization. Lag phase was noticed for 97-u-b and cas from day 0 to day 1, which implies slow initial increase in PV. In contrast, the rest of the samples did not exhibit a lag phase, indicating rapid accumulation of hydroperoxides. A decrease in PV was observed for g1, 82-s-a and 86-s-b from day 3 indicating that peroxides were decomposed to secondary oxidation products faster than new peroxides were formed. Similarly, hydroperoxide accumulation was significantly curtailed for 84-s-b, 104-p-g, and 105-p-g from day 7 to day 10. Overall, 97-u-b outperformed the rest of the peptides, as it consistently garnered the lowest PV throughout storage and was also comparable to cas from day 0 to day 7. The highest PV measured was for 84-s-b (101.67 meq O_2/kg oil) on day 7, and peak values were observed at this point for most samples. Furthermore, all samples exceeded the cut-off value for the peroxide value of oils (< 5 meq O_2/ kg oil).

3.3.2. Tocopherol consumption

Tocopherols (vitamin E) is the only antioxidant naturally present in
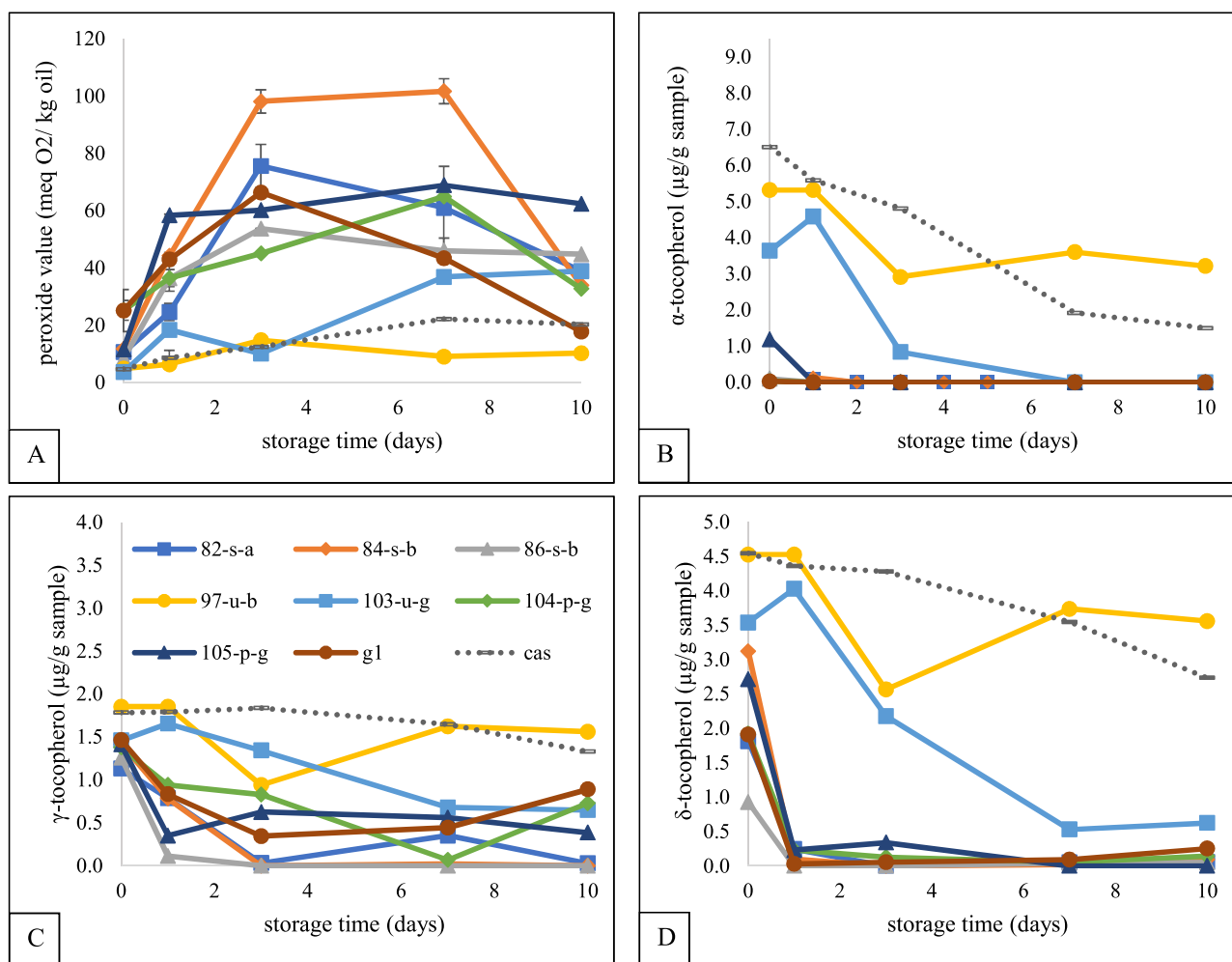

Fig. 3. A) Peroxide value (meq O_2/kg oil) and B-D) tocopherol content (α-, γ-, δ-tocopherol, respectively) of emulsions containing peptides or sodium caseinate during 10 days of storage room temperature. Blue is used for 82-s-a, orange is used for 84-s-b, gray is used for 86-s-b, yellow is used for 97-u-b, light blue is used for 103-u-g, green is used for 104-p-g, dark blue is used for 105-p-g, brown is used for g1, and dotted dark gray is used for cas.

oils from marine fish and its concentrations in refined fish oils are substantially lower than in most vegetable oils [18]. Tocopherols, especially α-tocopherol, exert their protective actions by interrupting autocatalytic reaction cycles by donating their phenolic hydrogen to peroxyl radicals, and by stabilization of preformed hydroperoxides [55]. Fig. 3B-D shows the evolution of tocopherols during a 10-day storage at room temperature. Tables S3–S5 in the Supplementary materials shows significant (p ≤ 0.05) differences between the samples and time points. For most of the samples (except 97-u-b, 103-p-g and cas), the α-tocopherol depleted rapidly already at day 0. This corresponds to those emulsions that were highly susceptible to oxidation and tocopherols were consumed as antioxidants.

The depletion of α-tocopherol in the 97-u-b emulsion was comparable to that in cas at day 10. It was also evident that emulsions with 97-u-b, 103-p-g and cas were the only samples that did not entirely consume α-tocopherol, which correlates well with the low formation of hydroperoxides (Fig. 3A). For γ- and δ-tocopherols, not much was consumed as compared to α-tocopherol. Calculations of % consumed tocopherol are shown in Table S6 and confirm the abovementioned interpretation of Fig. 3A. A common trend is that at least 25 % of the tocopherols were consumed for the rest of the samples. In line with this, α-tocopherol is superior amongst the others as it has two ortho methyl substituents, making it a stronger hydrogen donor than either β- or γ- (with only one ortho methyl substituent), as well as δ- which has no ortho methyl

substituent. This is in accordance with general accepted knowledge about activity of the different tocopherol homologs [36]. This order, however, is not always consistent and is affected by concentration of tocopherols [12,36].

3.3.3. Volatile secondary oxidation products

In the presence of transition metal ions (i.e., Fe^{+2}), unstable lipid hydroperoxides may decompose through the formation of peroxyl and alkoxyl radicals. It is generally accepted that volatile products are generated via fatty acid alkoxyl radicals. These alkoxyl radicals are cleaved by homolytic β-scission of the carbon-carbon bond on either side of the carbon carrying oxygen to form a broad spectrum of shorter-chain secondary oxidation volatiles [22,30]. Many of the volatiles identified in studies can be formed either by fragmentation of monohydroperoxides or by further oxidation of secondary oxidation products [18]. Based on the fatty acid composition of cod liver oil (Section 2.1), the n-9, n-6, n-3 series of fatty acids accounted for up to 28.80 %, 1.8 % and 20.30 % of the dominant fatty acids (FA), respectively. It is worth mentioning that t, t-2,4-heptadienal, 2-ethyl furan, and 1-penten-3-ol are products derived from n-3 PUFAs while t,t-2,4-decadienal is derived from n-6 PUFAs [27, 41,49]. Moreover, fish-like flavors present in rancid oils are mostly associated with the autoxidation of n-3 PUFAs [42].

In this study, the evolution of 5 out of 13 detected secondary oxidation volatiles (Fig. 4) will be discussed as these volatiles had a
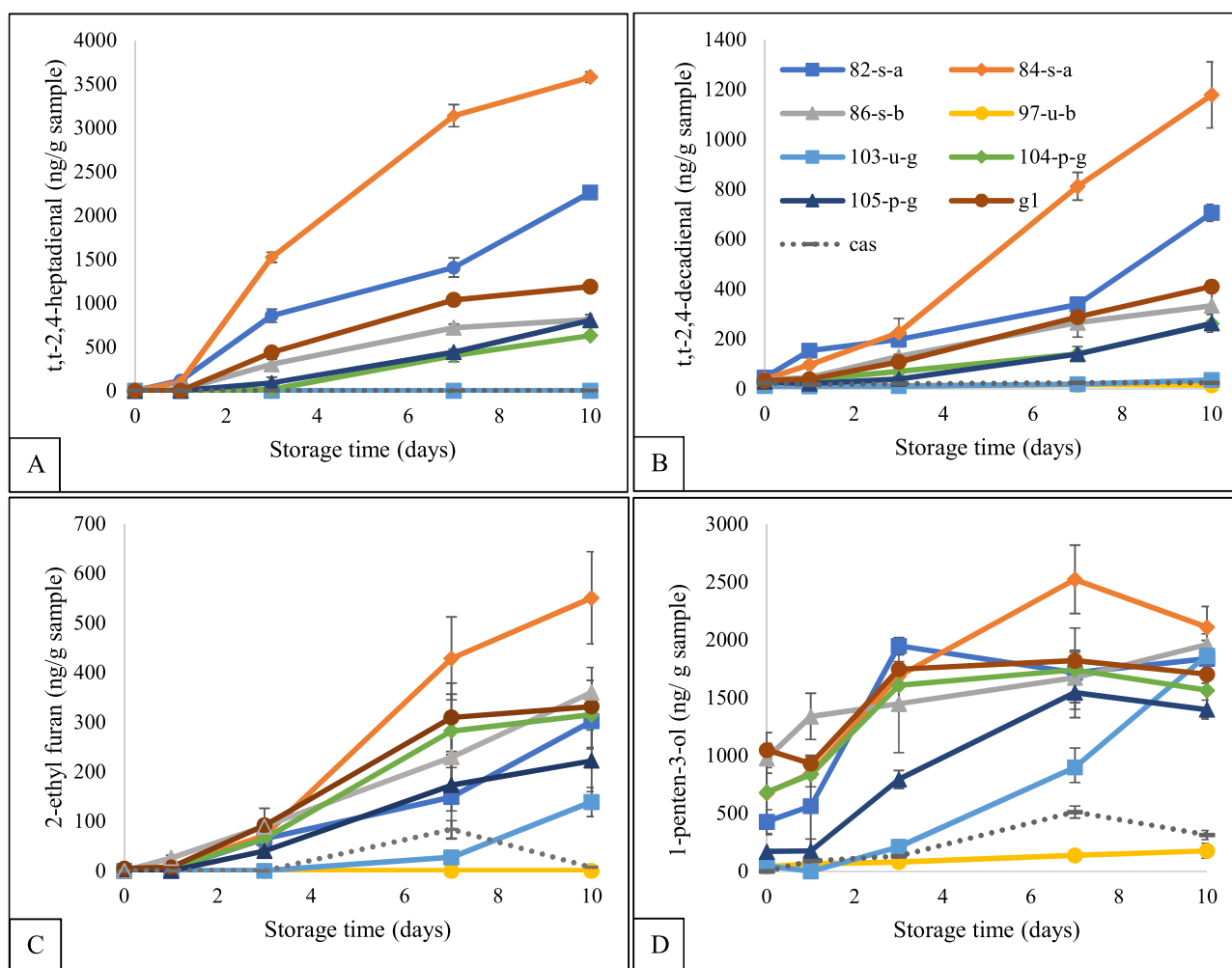
Fig. 4. Volatile secondary oxidation products (ng/g sample) A) t,t-2,4-heptadienal, B) t,t-2,4-decadienal, C) 2-ethylfuran, and D) 1-penten-3-ol formed in emulsions containing peptides or sodium caseinate during 10 days of storage at room temperature. Blue is used for 82-s-a, orange is used for 84-s-b, gray is used for 86-s-b, yellow is used for 97-u-b, light blue is used for 103-u-g, green is used for 104-p-g, dark blue is used for 105-p-g, brown is used for g1, and dotted dark gray is used for cas.

trend of gradual increase as time progressed. The evolution of the remaining compounds can be seen in Fig. S1 and Tables S7–11 in the Supplementary material. A general trend was observed for 84-s-b regarding the formation of volatile compounds. It was clear that for t, t-2,4-heptadienal, t,t-2,4-decadienal, 2-ethyl furan and 1-penten-3-ol, the 84-s-b emulsion had the highest concentration of these volatiles. This is aligned with the PV of this emulsion; 84-s-b peptide was inferior in terms of protecting the fish oil against oxidation. Overall, the emulsion stabilized with 97-u-b exhibited the highest oxidative stability and was comparable to cas at some instances (Fig. 4 and Fig. S1). Compounds t,t-2,4-heptadienal and 2-ethyl furan were not detected in the 97-u-b emulsion, while for 1-penten-3-ol, 97-u-b were detected in levels comparable to those in the cas emulsion. The 103-p-g emulsion showed comparable levels to 97-u-b and cas in terms of the formation of t,t-2,4-decadienal and t,t-2,4-heptadienal. These results can be confirmed by the slow depletion of alpha tocopherols by 103-p-g and relatively low PV at day 7 (36.88 meq O_2/kg oil), which implies that this emulsion was oxidatively stable and did not require the use of the tocopherols.

3.3.4. Emulsion color as an indication of lipid oxidation and non-enzymatic browning

The reaction of lipid oxidation products with amines, amino acids and proteins, (i.e., production of carbonyl compounds that leads to the formation of brown colored oxypolymers) has long been related to the browning observed in many fatty foods during processing and storage [20]. Non-enzymatic browning reactions can also be related to advanced stages of oxidation [41]. As shown in Table 3, 84-s-b, 97-u-b and cas were the lightest emulsions (higher *L values) while 105-p-g had a lower *L value indicating the darkest among others. 97-u-b and cas had lower red (*a); and blue (*b) values, which indicates that these samples had less yellow color compared to the rest of the samples. The *L, *a, *b values of 97-u-b and cas correlates with their high oxidative stability, hence lower tendency for lipid oxidation and non-enzymatic browning reactions to take place. The high *L of 84-s-b can possibly be explained by its small droplet size, meaning more light was transmitted. Among other factors, droplet size also affects color quantification [34]. One common thing amongst samples having lower *L, more negative *a, and higher *b is that these were the emulsions that had inferior oxidative stability. Most oxidized emulsions are darker brown due to advanced oxidation, which was also observed in a previous study on potato peptides [26].

The antioxidative properties of peptides are mainly related to their size, net charge, composition, structure and hydrophobicity [10,54]. The remarkable potency of 97-u-b for inhibiting lipid oxidation can at least be partly attributed to its positive charge that aids repulsion of positively charged metal ions from the interface, where the lipid oxidation is initiated [7]. Moreover, the positive net charge is a result of a high proportion of Lys (K) residues (4 of 16, i.e. 25 %), as observed in its AA sequence KVKINETVEIKGKFHV. The free amino group in K possesses a pair of free electrons and hence, has been suggested to chelate

pro-oxidative Fe (II) ions via electrostatic coordination [11]. It is also reported that the antioxidant properties of peptides can stem from the presence of Lys, Met, His, Trp and Tyr residues [50]. The presence of hydrophobic AAs (e.g., Ala, Leu, Val, Pro, Phe) has also been suggested to be important to promote peptide interaction with lipids resulting in an augmented radical scavenging ability [19,3]. [17] reported that the amino acid residue H in combination with hydrophobic (e.g., Leu, Pro, Val) or aromatic (Phe) amino acids may also contribute to high lipid peroxidation inhibition property. However, antioxidant activity of peptides cannot only be explained by the presence of certain AAs; their positioning and the sequential composition matters as well [65].

Peptide size also affects the potency of the peptides to retard lipid oxidation, where shorter peptides are generally attributed higher scavenging and lipid peroxidation inhibition activities compared to long-chain peptides [55]. In this study, 97-u-b had the second shortest sequence among the peptides (16 residues, MW= 1869.24 Da). Ren et al. [52] outlined that peptide chains containing < 3 kDa peptides were more of an effective scavenger of hydroxyl radical and inhibitor of lipid peroxidation when compared to chains containing > 3 kDa peptides. Moreover, good antioxidant properties were expected from 86-s-b as this was the shortest peptide (14 AAs). Its sequence ELQVSARVT-LEIEL contains multiple L residues, which is a hydrophobic AA that enhances the interaction of peptides with the lipophilic environment [19,3]. 86-s-b also contained multiple E residues, which is an electron donor, has chelating properties, and its presence increases the antioxidant capacity of peptides [3]. Among other negatively charged peptides, 86-s-b provided the highest oxidative stability, which could be due to the factors such as its size and presence of E and L AAs that contributed to its ability to inhibit lipid oxidation. On the other hand, overall negative net charge hindered the oxidative stability. This signifies the complexity of peptide antioxidant activity.

The low oxidative stability of 84-s-b is highly likely related to the highly negative net charge of this peptide at pH 7 (Table 1) that favored attraction of metal ions to the interface catalyzing lipid oxidation. Although 84-s-b has multiple hydrophobic residues (i.e. A, L, V, G, F) in its AA sequence (VGFACSGSAQTYLSFEGDNTGRGEEEVAI) that promotes peptide interaction with lipids, the positioning of the AAs in the sequence may also have affected its antioxidant power [51]. Moreover, it is also noteworthy that g1 has a low oxidative stability, reaching as high as 66.38 meq O_2/kg oil on day 3. Even though the g1 emulsion exhibited excellent physical stability, this sample had a dramatic increase in PV from day 0 to day 3. This is in line with previous studies, where g1 samples showed low oxidative stability (i.e., highest generation of PBN-lipid spin adducts) [24] and reaching peak PV level at day 3 when used as an emulsifier in a low-fat emulsion [26]. Furthermore, it must be kept in mind that the overall antioxidative activity must be ascribed to the integrative effects of these actions rather than to individual actions of peptides [10]. For example, when a smaller droplet size, which yields to larger oil-water interfacial area, is combined with high negative net charge, which attracts positively charged metal ions towards the interface, this combination may lead to higher levels of lipid oxidation if the peptides do not have good antioxidant properties.

Overall, oxidative stability of the positively charged peptides (97-u-b and 103-p-g) were the most comparable to cas, which is negatively charged at pH 7 and shows excellent metal chelating and good radical scavenging activity. The remarkable oxidative stability of 97-u-b, and to some extent 103-p-g, could be presumably attributed to repulsion of the metal ions at the oil-water interface. This agrees with previous results indicating that positively charged peptides considerably reduce lipid oxidation in emulsions when accelerated by the addition of ferrous ions [26].

4. Conclusions

Functional peptides derived from seaweed, bacterial and potato protein with emulsifying properties can be identified using

Table 3
Color *L, *a, *b of the emulsions stabilized with different peptides and sodium caseinate at day 10 under storage at room temperature.

Sample	*L	*a	*b
82-s-a	84.7[c]	-6.0[a]	11.6[cd]
84-s-b	86.8[de]	-5.7[ab]	12.9[de]
86-s-b	86.4[d]	-5.6[bc]	14.1[e]
97-u-b	87.6[e]	-4.9[ef]	7.1[ab]
103-u-g	85.0[c]	-5.3[cde]	11.3[cd]
104-p-g	83.1[b]	-5.4[bcd]	11.3[cd]
105-p-g	76.7[a]	-5.1[de]	9.3[bc]
g1	84.3[c]	-5.2[de]	12.8[de]
Cas	87.2[de]	-4.7[f]	5.4[a]

Values are presented as means (n = 9). Means followed by the same letter/s per sample are not significantly different (p ≤ 0.05).

bioinformatics tools. The dual functional role of a peptide to be an emulsifier and antioxidant in an emulsion system can be positively exploited. Among the 11 peptides evaluated, the favorable peptides in terms of conferring good emulsion stability were 82-s-a, 84-s-b, 86-s-b, 97-u-b,104-p-g and g1 based on their highly negative zeta potential, creaming stability and small oil droplets throughout storage. It was shown that the secondary structure of the peptides changed to more α-helical (up to 55 %) or β-strand (up to 70 %) structures when adsorbed at the oil-water interface compared to their disordered structure in solution (e.g., from 4 % α-helical or 42 % β-strand). Several factors, such as peptides' charge, length, secondary structure, ability to reduce oil-water interfacial tension, amino acid composition, were investigated in this study and shown to affect emulsion formation and stability. However, factors such as other structural characteristics, adsorption kinetics, surface coverage and emulsifier concentration, homogenizers used, and processing conditions can also have an effect which needs to be further investigated. Another aspect that was investigated was the oxidative stability of the peptide-based emulsions. In this context, 97-u-b exhibited superior antioxidant properties, as it had the lowest peroxide value, tocopherol consumption, concentration of volatile products and incidence of non-enzymatic browning. The peptide's mode of action in retarding lipid oxidation is attributed to several parameters such as its charge, composition, structure, and hydrophobicity; 97-u-b is a positively charged short chain peptide that not only has hydrophobic AAs that enhances radical scavenging activity but also multiple K residues that chelates Fe (II) ions. Moreover, the total antioxidant capacity is a collective consequence of the aforementioned factors rather than the individual effects of the amino acids. Altogether, 97-u-b was the best performing peptide in both the physical and oxidative stability analyses followed by 103-u-g.

Although synthetic peptides were used in this study, the predicted peptides embedded within each abovementioned protein source would prove to be a clean and natural alternative to synthetic surfactants. Our study provides novel insight into the relation between physical and oxidative stability of emulsions, peptide dual functionality, interfacial peptide conformation and structural dynamics during emulsion production. This new molecular insight allows designing targeted enzymatic hydrolysis, which leads to release of peptides and downstream purification or direct application as a functional food ingredient. It is also worth noting that identification of emulsifier peptides by using proteomics and bioinformatics followed by the validation of their functionality in food model systems (e.g., oil-in-water emulsions) allow to design a targeted-hydrolysis process of the parent protein for the industrial production of these peptides by enzymatic processes.

CRediT authorship contribution statement

Betül Yesiltas: Conceptualization, Methodology, Formal analysis, Investigation, Visualization, Writing – original draft. **Alyssa M. Soria Caindec:** Formal analysis, Investigation. **Pedro J. García-Moreno**: Conceptualization, Methodology, Formal analysis, Investigation, Writing – review & editing. **Simon Gregersen:** Methodology, Formal analysis, Visualization, Writing – review & editing. **Tobias H. Olsen:** Conceptualization, Formal analysis, Investigation. **Nykola C. Jones:** Methodology, Formal analysis, Writing – review & editing. **Søren V. Hoffmann:** Methodology, Writing – review & editing. **Paolo Marcatili:** Conceptualization, Methodology, Formal analysis, Investigation. **Michael T. Overgaard:** Conceptualization, Funding acquisition. **Egon B. Hansen:** Conceptualization, Funding acquisition, Project administration. **Charlotte Jacobsen**: Conceptualization, Methodology, Funding acquisition, Project administration, Supervision, Writing – review & editing.

Declaration of Competing Interest

The authors declare that they have no known competing financial interests or personal relationships that could have appeared to influence the work reported in this paper.

Data Availability

Data will be made available on request.

Acknowledgements

Appendix A. Supporting information

Supplementary data associated with this article can be found in the online version at doi:10.1016/j.colsurfa.2023.131069.

References

[1] A. Abdul-Gader, A.J. Miles, B.A. Wallace, A reference dataset for the analyses of membrane protein secondary structures and transmembrane residues using circular dichroism spectroscopy, Bioinformatics 27 (12) (2011) 1630–1636, https://doi.org/10.1093/bioinformatics/btr234.

[2] R. Ait-Akbour, P. Boustingorry, F. Leroux, F. Leising, C. Taviot-Guého, Adsorption of polycarboxylate poly (ethylene glycol) (PCP) esters on montmorillonite (Mmt): effect of exchangeable cations (Na+, Mg2+ and Ca2+) and PCP molecular structure, J. Colloid Interface Sci. 437 (2015) 227–234, https://doi.org/10.1016/j.jcis.2014.09.027.

[3] R.E. Aluko, Amino acids, peptides, and proteins as antioxidants for food preservation, in: Handbook of Antioxidants for Food Preservation, 2015, pp. 105–140, https://doi.org/10.1016/B978-1-78242-089-7.00005-1.

[4] N.J. Anthis, G.M. Clore, Sequence-specific determination of protein and peptide concentrations by absorbance at 205 nm, Protein Sci. 22 (6) (2013) 851–858, https://doi.org/10.1002/pro.2253.

[5] N. Arunkumar, M. Deecaraman, C. Rani, Nanosuspension technology and its applications in drug delivery, Asian J. Pharm. (AJP): Free Full Text. Artic. Asian J. Pharm. 3 (3) (2009), https://doi.org/10.22377/AJP.V3I3.261.

[6] O. Benjamin, P. Silcock, J. Beauchamp, A. Buettner, D.W. Everett, Emulsifying properties of legume proteins compared to β-lactoglobulin and Tween 20 and the volatile release from oil-in-water emulsions, J. Food Sci. 79 (10) (2014) E2014–E2022, https://doi.org/10.1111/1750-3841.12593.

[7] C.C. Berton-Carabin, M.H. Ropers, C. Genot, Lipid oxidation in oil-in-water emulsions: involvement of the interfacial layer, Compr. Rev. Food Sci. Food Saf. 13 (5) (2014) 945–977, https://doi.org/10.1111/1541-4337.12097.

[8] E.G. Bligh, W.J. Dyer, A rapid method of total lipid extraction and purification, Can. J. Biochem. Physiol. 37 (8) (1959) 911–917, https://doi.org/10.1139/o59-099.

[9] A. Can Karaca, N.H. Low, M.T. Nickerson, Potential use of plant proteins in the microencapsulation of lipophilic materials in foods, Trends Food Sci. Technol. 42 (1) (2015) 5–12, https://doi.org/10.1016/j.tifs.2014.11.002.

[10] H.M. Chen, K. Muramoto, F. Yamauchi, K. Fujimoto, K. Nokihara, Antioxidative properties of histidine-containing peptides designed from peptide fragments found in the digests of a soybean protein, J. Agric. Food Chem. 46 (1) (1998) 49–53, https://doi.org/10.1021/jf970649w.

[11] Y. Cheng, J. Chen, Y.L. Xiong, Interfacial adsorption of peptides in oil-in-water emulsions costabilized by tween 20 and antioxidative potato peptides, J. Agric. Food Chem. 62 (47) (2014) 11575–11581, https://doi.org/10.1021/jf5038135.

[12] C. Chotimarkorn, S. Benjakul, N. Silalai, Antioxidant components and properties of five long-grained rice bran extracts from commercial available cultivars in Thailand, Food Chem. 111 (3) (2008) 636–641, https://doi.org/10.1016/j.foodchem.2008.04.031.

[13] R.J.B.M. Delahaije, L.M.C. Sagis, J. Yang, Impact of particle sedimentation in pendant drop tensiometry, Langmuir 38 (33) (2022) 10183–10191, https://doi.org/10.1021/acs.langmuir.2c01193.

[14] A.F. Dexter, A.P.J. Middelberg, Switchable peptide surfactants with designed metal binding capacity, J. Phys. Chem. C 111 (28) (2007) 10484–10492, https://doi.org/10.1021/jp071554s.

[15] A.F. Dexter, A.P.J. Middelberg, Peptides as functional surfactants, Ind. Eng. Chem. Res. 47 (17) (2008) 6391–6398, https://doi.org/10.1021/ie800127f.

[16] E. Dickinson, Towards more natural emulsifiers, Trends Food Sci. Technol. 4 (10) (1993) 330–334, https://doi.org/10.1016/0924-2244(93)90103-H.

[17] X. Duan, D. Ocen, F. Wu, M. Li, N. Yang, J. Xu, H. Chen, L. Huang, Z. Jin, X. Xu, Purification and characterization of a natural antioxidant peptide from fertilized

eggs, Food Res. Int. 56 (2014) 18–24, https://doi.org/10.1016/j.foodres.2013.12.016.

[18] E. Kulås, Antioxidant Properties of Tocopherols in Fish Oils (Graduate Thesis and Dissertation), Dalhousie Unversity Daltech, 2000.

[19] A. Egusa Saiga, T. Nishimura, Antioxidative properties of peptides obtained from porcine myofibrillar proteins by a protease treatment in an Fe (II)-induced aqueous lipid peroxidation system, Biosci. Biotechnol. Biochem. 77 (11) (2013) 2201–2204, https://doi.org/10.1271/bbb.130369.

[20] B. El-Zeany, L.E. Fattah, Oxidised lipids-proteins browning reaction. Part 6. Browning produced by the interaction of free fatty acids with proteins, Grasas Aceites 33 (1982) 216–219, https://doi.org/10.3989/gya.2000.v51.i1-2.405.

[21] M. Enser, G.B. Bloomberg, C. Brock, D.C. Clark, De novo design and structure-activity relationships of peptide emulsifiers and foaming agents, Int. J. Biol. Macromol. 12 (2) (1990) 118–124, https://doi.org/10.1016/0141-8130(90)90063-G.

[22] E.N. Frankel, Lipid Oxidation, Oily Press, Dundee, 1998.

[23] Frankel, E. N. (2012). Lipid Oxidation, Woodhead Publishing Limited, 2012.

[24] P.J. García-Moreno, C. Jacobsen, P. Marcatili, S. Gregersen, M.T. Overgaard, M. L. Andersen, E.B. Hansen, et al., Emulsifying peptides from potato protein predicted by bioinformatics: stabilization of fish oil-in-water emulsions, Food Hydrocoll. 101 (2020), https://doi.org/10.1016/j.foodhyd.2019.105529.

[25] P.J. García-Moreno, S. Gregersen, E.R. Nedamani, T.H. Olsen, P. Marcatili, M. T. Overgaard, C. Jacobsen, Identification of emulsifier potato peptides by bioinformatics: application to omega-3 delivery emulsions and release from potato industry side streams, Sci. Rep. 10 (1) (2020) 690, https://doi.org/10.1038/s41598-019-57229-6.

[26] P.J. García-Moreno, J. Yang, S. Gregersen, N.C. Jones, C.C. Berton-Carabin, L.M. C. Sagis, C. Jacobsen, et al., The structure, viscoelasticity and charge of potato peptides adsorbed at the oil-water interface determine the physicochemical stability of fish oil-in-water emulsions, Food Hydrocoll. 115 (2021), 106605, https://doi.org/10.1016/j.foodhyd.2021.106605.

[27] I. Giogios, K. Grigorakis, I. Nengas, S. Papasolomontos, N. Papaioannou, M. N. Alexis, Fatty acid composition and volatile compounds of selected marine oils and meals, J. Sci. Food Agric. 89 (1) (2009) 88–100, https://doi.org/10.1002/jsfa.3414.

[28] I. Goldberg, R. Williams, Biotechnology and Food Ingredients, Chapman and Hall, London, 1991.

[29] S. Gregersen, M. Pertseva, P. Marcatili, S.V. Holdt, C. Jacobsen, P.J. García-Moreno, E.B. Hansen, M.T. Overgaard, Proteomic characterization of pilot scale hot-water extracts from the industrial carrageenan red seaweed *Eucheuma denticulatum*, Algal Res. 62 (2022), 102619, https://doi.org/10.1016/j.algal.2021.102619.

[30] Grosch, W. (1987). Reactions of hydroperoxides – products of low molecular weight. In: Autoxidation of Unsaturated Lipids (pp. 95-139). London: Academic Press.

[31] G. Hasenheuttl, R. Hartel. Food Emulsifier and Their Applications, 2nd ed., 2008, https://doi.org/10.1007/978-0-387-75284-6.

[32] S.V. Hoffmann, M. Fano, M. van de Weert. Circular Dichroism Spectroscopy for Structural Characterization of Proteins, 2016, https://doi.org/10.1007/978-1-4939-4029-5_6.

[33] A.F. Horn, N.S. Nielsen, U. Andersen, L.H.S. Jensen, A. Horsewell, C. Jacobsen, The choice of homogenisation equipment affects lipid oxidation in emulsions, Food Chemistry 134 (2012) 803–810.

[34] Y.T. Hu, Y. Ting, J.Y. Hu, S.C. Hsieh, Techniques and methods to study functional characteristics of emulsion systems, J. Food Drug Anal. 25 (1) (2017) 16–26, https://doi.org/10.1016/j.jfda.2016.10.021.

[35] C. Jacobsen, Some strategies for the stabilization of long chain n-3 PUFA-enriched foods: a review, Eur. J. Lipid Sci. Technol. 117 (2015) 1853–1866, https://doi.org/10.1002/ejlt.201500137.

[36] A. Kamal-Eldin, L.Å. Appelqvist, The chemistry and antioxidant properties of tocopherols and tocotrienols, Lipids 31 (7) (1996) 671–701, https://doi.org/10.1007/BF02522884.

[37] I. Kralova, J. Sjöblom, Surfactants used in food industry: a review, J. Dispers. Sci. Technol. 30 (9) (2009) 1363–1383, https://doi.org/10.1080/01932690902735561.

[38] K.E. Krebs, M.C. Phillips, The contribution of α-helices to the surface activities of proteins, FEBS Lett. 175 (2) (1984) 263–266, https://doi.org/10.1016/0014-5793(84)80748-6.

[39] R.S.H. Lam, M.T. Nickerson, Food proteins: a review on their emulsifying properties using a structure–function approach, Food Chem. 141 (2) (2013) 975–984, https://doi.org/10.1016/j.foodchem.2013.04.038.

[40] C. Le Visage, M. Deyme, S. Yoshikawa, The influence of the helicity of soluble peptides on their adsorption kinetics, Colloids Surf. B: Biointerfaces 9 (5) (1997) 233–238, https://doi.org/10.1016/S0927-7765(97)00028-3.

[41] F.S.H. Lu, N.S. Nielsen, C.P. Baron, C. Jacobsen, Oxidative degradation and non-enzymatic browning due to the interaction between oxidised lipids and primary amine groups in different marine PL emulsions, Food Chem. 135 (4) (2012) 2887–2896, https://doi.org/10.1016/j.foodchem.2012.07.008.

[42] H. Maarse, Volatile Compounds in Foods and Beverages, Marcel Dekker, New York, 1991.

[43] D.J. McClements. Food Emulsions: Principles, Practice, and Techniques, 3rd ed., CRC Press, Boca Raton, Florida, USA, 2015.

[44] D.J. McClements, C.E. Gumus, Natural emulsifiers — biosurfactants, phospholipids, biopolymers, and colloidal particles: molecular and physicochemical basis of functional performance, Adv. Colloid Interface Sci. 234 (2016) 3–26, https://doi.org/10.1016/j.cis.2016.03.002.

[45] A.J. Miles, B.A. Wallace, Circular dichroism spectroscopy of membrane proteins, Chem. Soc. Rev. 45 (2016) 4859–4872, https://doi.org/10.1039/c5cs00084j.

[46] A.J. Miles, F. Wien, B.A. Wallace, Redetermination of the extinction coefficient of camphor-10-sulfonic acid, a calibration standard for circular dichroism spectroscopy, Anal. Biochem. 335 (2) (2004) 338–339, https://doi.org/10.1016/j.ab.2004.08.035.

[47] B. Nordén, A. Rodger, T. Dafforn, Linear Dichroism and Circular Dichroism: A Textbook on Polarized-light Spectroscopy, The Royal Society of Chemistry, Cambridge, 2010.

[48] B. Ozturk, D.J. McClements, Progress in natural emulsifiers for utilization in food emulsions, Curr. Opin. Food Sci. 7 (2016) 1–6, https://doi.org/10.1016/j.cofs.2015.07.008.

[49] X.-Q. Pan, H. Ushio, T. Ohshima, Comparison of volatile compounds formed by autoxidation and photosensitized oxidation of cod liver oil in emulsion systems, Fish. Sci. 71 (2005) 639–647, https://doi.org/10.1111/j.1444-2906.2005.01010.x.

[50] E.A. Peña-Ramos, Y.L. Xiong, Antioxidative activity of whey protein hydrolysates in a liposomal system, J. Dairy Sci. 84 (12) (2001) 2577–2583, https://doi.org/10.3168/jds.S0022-0302(01)74711-X.

[51] N. Rajapakse, E. Mendis, W.K. Jung, J.Y. Je, S.K. Kim, Purification of a radical scavenging peptide from fermented mussel sauce and its antioxidant properties, Food Res. Int. 38 (2) (2005) 175–182, https://doi.org/10.1016/j.foodres.2004.10.002.

[52] J. Ren, M. Zhao, J. Shi, J. Wang, Y. Jiang, C. Cui, Y. Kakuda, S.J. Xue, Purification and identification of antioxidant peptides from grass carp muscle hydrolysates by consecutive chromatography and electrospray ionization-mass spectrometry, Food Chem. 108 (2) (2008) 727–736, https://doi.org/10.1016/j.foodchem.2007.11.010.

[53] M. Saito, M. Ogasawara, K. Chikuni, M. Shimizu, Synthesis of a peptide emulsifier with an amphiphilic structure, Biosci. Biotechnol. Biochem. 59 (3) (1995) 388–392, https://doi.org/10.1271/bbb.59.388.

[54] B.H. Sarmadi, A. Ismail, Antioxidative peptides from food proteins: a review, Peptides 31 (10) (2010) 1949–1956, https://doi.org/10.1016/j.peptides.2010.06.020.

[55] F. Shahidi, Antioxidants: principles and applications, in: Handbook of Antioxidants for Food Preservation, Woodhead Publishing, Cambridge, 2015, pp. 1–14.

[56] N.C. Shantha, E.A. Decker, Rapid, sensitive, iron-based spectrophotometric methods for determination of peroxide values of food lipids, J. AOAC Int. 77 (2) (1994) 421–424.

[57] M. Shimizu, M. Saito, Lipid-protein interaction at an emulsified oil surface: protein structures and their roles in lipid binding, ACS Symp. Ser. 650 (1996) 156, https://doi.org/10.1021/bk-1996-0650.ch013.

[58] P. Smulders, Formation and Stability of Emulsions Made with Proteins and Peptides (Graduate Thesis and Dissertation), Wageningen University, 2000.

[59] N. Sreerama, R.W. Woody, Estimation of protein secondary structure from circular dichroism spectra: comparison of CONTIN, SELCON, and CDSSTR methods with an expanded reference set, Anal. Biochem. 287 (2) (2000) 252–260, https://doi.org/10.1006/abio.2000.4880.

[60] C. Stauffer, Emulsifiers, Eagan Press, St Paul, 1999.

[61] I. Tavernier, W. Wijaya, P. Van der Meeren, K. Dewettinck, A.R. Patel, Food-grade particles for emulsion stabilization, Trends Food Sci. Technol. 50 (2016) 159–174, https://doi.org/10.1016/j.tifs.2016.01.023.

[62] B. Wang, L. Li, C.-F. Chi, J.-H. Ma, H.-Y. Luo, Y. Xu, Purification and characterisation of a novel antioxidant peptide derived from blue mussel (Mytilus edulis) protein hydrolysate, Food Chem. 138 (2–3) (2013) 1713–1719, https://doi.org/10.1016/j.foodchem.2012.12.002.

[63] L. Whitmore, B.A. Wallace, Protein secondary structure analyses from circular dichroism spectroscopy, Methods Ref. Databases 89 (2007) 392–400, https://doi.org/10.1002/bip.20853.

[64] B. Yesiltas, S. Gregersen, L. Lægsgaard, M.L. Brinch, T.H. Olsen, P. Marcatili, M. T. Overgaard, E.B. Hansen, C. Jacobsen, P.J. García-Moreno, Emulsifier peptides derived from seaweed, methanotrophic bacteria, and potato proteins identified by quantitative proteomics and bioinformatics, Food Chem. 362 (February) (2021), 130217, https://doi.org/10.1016/j.foodchem.2021.130217.

[65] B. Yesiltas, P.J. García-Moreno, S. Gregersen, T.H. Olsen, N.C. Jones, S. v Hoffmann, P. Marcatili, M.T. Overgaard, E.B. Hansen, C. Jacobsen, Antioxidant peptides derived from potato, seaweed, microbial and spinach proteins: oxidative stability of 5 % fish oil-in-water emulsions, Food Chem. 385 (2022), 132699, https://doi.org/10.1016/j.foodchem.2022.132699.